Latin American Journal of Aquatic Research, 54(3): 508-519, 2026
DOI: 10.3856/vol54-issue3-fulltext-3613

Short Communication

Microphytoplankton communities associated with deep thermoclines in the southwestern Gulf of Mexico during a "Nortes" storm season

Elizabeth Durán-Campos[1], David Alberto Salas-de-León[2]
María Adela Monreal-Gómez[2] & Erik Coria-Monter[2]
[1]Escuela Nacional de Ciencias de la Tierra, Universidad Nacional Autónoma de México
Copilco, Coyoacán, Ciudad de México, México
[2]Instituto de Ciencias del Mar y Limnología, Universidad Nacional Autónoma de México
Copilco, Coyoacán, Ciudad de México, México
Corresponding author: Erik Coria-Monter (coria@cmarl.unam.mx)

ABSTRACT. The ocean thermocline acts as a critical transition layer that regulates the vertical distribution of chemical compounds and microorganisms. Because its depth is highly variable, ranging from a few meters to over 100 m, it influences the vertical distribution of species. This study evaluates microphytoplankton communities associated with deep thermoclines off the coast of Veracruz in the southwestern Gulf of Mexico. Data and samples were collected during a multidisciplinary research cruise in February 2023, coinciding with a "Nortes" storm season. Using a CTD-Rosette system, we obtained high-resolution hydrographic profiles and water samples for taxonomic analysis. Our results identified deep thermoclines (ranging from 80 to 140 m depth) that supported a total of 110 species across all sampling stations, comprising 57 diatoms, 48 dinoflagellates, 2 cyanobacteria, 2 silicoflagellates, and 1 ciliate. Diatoms were the most abundant group (20,060 cells L^{-1}), followed by dinoflagellates (17,720 cells L^{-1}). *Mesodinium rubrum*, *Pseudo-nitzschia pseudodelicatissima*, *Trichodesmium hildebrandtii*, *Heterocapsa orientalis*, and *Dictyocha fibula* emerged as the most abundant taxa. Ecological indices, including Margalef richness (D_{Mg} = 10.17) and Shannon-Weaver diversity (*H'* = 4.03), indicate high community complexity, confirming that the thermocline serves a pivotal niche for microphytoplankton. These findings enhance our oceanographic understanding of the southwestern Gulf of Mexico by characterizing microphytoplankton at specific depths during a season that has historically been underrepresented in research due to the navigational challenges posed by stormy weather.

Keywords: microphytoplankton taxonomic composition; thermocline; winter storm season; Veracruz; Gulf of Mexico

Phytoplankton comprises a highly diverse community of microorganisms distributed throughout the euphotic layer of the world ocean (Vajravelu et al. 2017). While primarily composed of autotrophic species, it also includes significant numbers of mixotrophic and even heterotrophic organisms (Reynolds 2006). This community provides vital ecosystem services, most notably oxygen production and carbon sequestration through photosynthesis (Siegel et al. 2023). Furthermore, as the base of the marine food web, phytoplankton supports high-value ecological species (Grigoratou et al. 2025). Besides, by occupying the lowest trophic levels, they sustain major global fisheries, including sardine, anchovy, and herring populations (Grigoratou et al. 2025).

Associate Editor: José Luis Iriarte

Due to their planktonic nature, phytoplankton distributions are largely dictated by hydrodynamic processes and vertical thermal gradients. In the ocean, temperature varies significantly with depth, establishing the thermocline, a stable vertical gradient that separates warm surface waters from colder, denser deep layers (Pedlosky 2006, Alvarez et al. 2021). The thermocline exhibits pronounced seasonal fluctuations; for example, in the Northern Hemisphere, intense summer irradiance promotes a shallow, well-defined thermocline, whereas winter cooling and mechanical winds stress induce convective mixing that deepens this layer (Xu et al. 2017), potentially impacting biological communities.

For phytoplankton, the thermocline is a critical ecological determinant. The resulting thermal gradient can segregate distinct communities: those adapted to the high-irradiance, warmer surface waters, and those specialized for the colder, nutrient-rich deeper layers (Mena et al. 2019). This vertical partitioning has been documented globally, including the western English Channel (Sharples et al. 2001), the eastern Mediterranean Sea (Vidussi et al. 2001), the Celtic Sea (Hickman et al. 2009), and the Agulhas Bank (Carter et al. 2010).

In the Gulf of Mexico, a large, semi-enclosed sea of the North American continent, research on phytoplankton has evolved through several scientific phases. Early studies focused primarily on taxonomic characterization (e.g. Licea et al. 2004, 2011, 2017), while more contemporary efforts have shifted toward evaluating the role of hydrodynamic processes in governing community composition, distribution, and abundance (e.g. Durán-Campos et al. 2017, 2025, González-Fernández et al. 2025).

Along the southwestern Gulf of Mexico coast, the coast off Veracruz is particularly noteworthy. This area has been a focal point for intensive physical and biological investigation. It is recognized as a biological hotspot (Salas-Pérez & Granados-Barba 2008) characterized by exceptionally high phytoplankton diversity and biomass. For example, early studies identified 46 species of dinoflagellates of the genus *Protoperidinium*, 33 species of *Ceratium* (currently recognized as *Tripos*), and 38 species within the order Dinophysiales, establishing essential taxonomic keys for regional identification (Okolodkov 2008, 2010, 2014). Furthermore, comprehensive inventories have documented up to 275 species, revealing significant seasonal pulse dynamics in species richness. These studies indicate that species diversity peaks during June and October, while reaching its annual minima in April, November, and December (Okolodkov et al. 2011).

While phytoplankton research off the coast of Veracruz has been important to our ecological understanding of the region, significant gaps persist. To date, the majority of research has focused on taxonomic characterization and morphological descriptions. Although these inventories constitute relevant regional data, they often overlook the intricate coupling between the biota and the physical environment.

Consequently, the influence of the water column's physical structure on phytoplankton communities remains understudied. There is a lack of data regarding taxonomic composition at specific vertical strata; in particular, the community structure within the thermocline remains poorly understood. As a distinct thermal transition zone, the thermocline acts as a physical and chemical barrier that may harbor unique species assemblages distinct from those in the surface layer (Wang et al. 2024). Therefore, integrating depth-specific sampling is essential for a comprehensive understanding of the ecological dynamics in the region off the coast of Veracruz.

Furthermore, existing characterizations of regional phytoplankton exhibit a pronounced temporal bias. Indeed, scientific literature has focused predominantly on the warm spring and summer seasons. In contrast, the ecological processes of the cold winter season have been largely neglected. This period is of particular oceanographic interest, as the passage of cold fronts and storm events defines it. These phenomena drastically alter the vertical structure of the water column by inducing vertical mixing and deepening the thermocline (López-Cabello et al. 2025), environmental shifts that phytoplankton communities must fundamentally adapt to.

In this context, the study identifies the microphytoplankton species associated with deep thermoclines off the coast of Veracruz in the southwestern Gulf of Mexico during the 2023 "Nortes" storm season. By focusing on this dynamic hydrographic feature, we aim to elucidate how vertical stratification influences community structure during periods of intense atmospheric forcing.

To move beyond a purely descriptive taxonomic list, this study incorporates ecological indices, both species richness and diversity, to provide a robust ecological interpretation of the thermocline's role. Calculating species richness allows us to quantify the biological inventory supported by the subsurface layers, while diversity indices provide insight into the community's evenness and stability.

These metrics are essential for determining whether the thermocline acts as a specialized niche that concen-

trates unique species or as a high-biodiversity refuge that maintains ecosystem resilience against the turbulent mixing characteristic of the "Nortes" season. Through this lens, the thermocline is evaluated not just as a physical barrier, but as a critical driver of biological complexity in the southwestern gulf.

To fulfill the academic objectives of this study, a multidisciplinary research cruise (ACGOM-1) was conducted from February 3 to 13, 2023, aboard the R/V Justo Sierra (UNAM). The study focused on the waters off the coast of Veracruz (19º00'-19º20'N; 96º15'-95º45'W) (Fig. 1), a region characterized by complex hydrodynamics and three distinct climatic phases. According to the seasonal classifications by Salas-Monreal et al. (2022), the cruise took place during the northerly wind season (September-April), which is followed by a dry season (May-June) and a subsequent rainy season (July-August). In terms of physical dynamics, this region is defined by persistent vertical stratification. Previous studies indicate that oceanographic fronts are present at least 35% of the year (Salas-Monreal et al. 2019). These features, combined with the seasonal wind patterns, create a highly variable environment that significantly influences the local distribution of physical and biological properties.

Hydrographic data and water samples were collected at six stations (Fig. 1) using a General Oceanics rosette system equipped with 12 Niskin bottles (10 L). The rosette was integrated with a Sea-Bird 911 plus CTD (conductivity-temperature-depth) profiler, featuring an SBE 43 dissolved oxygen sensor and a WET Labs ECO fluorescence sensor; all instruments were factory-calibrated before the cruise. At each station, hydrographic profiles were recorded at a sampling frequency of 24 Hz, spanning from the sea surface to approximately 5 m above the seafloor.

During each CTD cast, the thermocline depth was identified by locating the maximum vertical temperature gradient. Water samples were then selectively collected at these discrete depths to characterize the associated microphytoplankton community. Samples were immediately fixed with Lugol's iodine solution and stored in the dark (Edler & Elbrächter 2010) until laboratory analysis. It should be noted that the samples collected represent a single cast at each station rather than replicated collections.

Microphytoplankton were quantified using the Utermöhl technique (Edler & Elbrächter 2010). Samples were settled in 50 mL sedimentation columns for 24 h before examination with a Carl Zeiss Axiovert A1 inverted microscope. To ensure taxonomic precision, the entire base of the sedimentation column was scanned at multiple magnifications (20x, 40x, and 100x), enabling observation of minute morphological diagnostic features. Organisms were identified to the lowest taxonomic level (species) using specialized regional and global keys (e.g. Cupp 1943, Komárek & Anagnostidis 1986, Throndsen 1997, Tomas 1997, Throndsen et al. 2003). Finally, raw counts were standardized to cell abundance (cells L^{-1}) according to established protocols (Edler & Elbrächter 2010).

Initial processing of the CTD data was conducted using the manufacturer's software (SBE Data Processing v7.26.7). After applying filters to remove noise and spurious data, the measurements were bin-averaged to 1-decibar intervals. Standard algorithms were then used to derive temperature (°C) and density (kg m^{-3}).

To evaluate the microphytoplankton community, we employed several ecological indices, primarily the Margalef species richness index (D_{Mg}) and the Shannon-Weaver diversity index (H'). The Margalef index was calculated according to Margalef (1969), $D_{Mg} = (\mathrm{S} - 1)/\ \mathrm{Ln}(\mathrm{N})$, where S is the total number of species and N is the total number of individuals. In this context, values <2 indicate low biodiversity, 2-3 indicate moderate richness, and values >3 indicate high species diversity. The Shannon-Weaver index (H') was calculated following the expression provided by Ortiz-Burgos (2016), $H' = -\sum_{n=1}^{n}(\mathrm{pi} \times \mathrm{Ln}\ \mathrm{p_i})$, where pi is the proportion of each group in the sample, and Ln pi is the natural logarithm of this proportion. Values generally range from 0 to >3.5, where higher values indicate greater diversity and stability. As noted by Magurran (2004), H', it is a widely utilized metric for comparing habitat diversity and quantifying biological variability. All indices were computed using the ''biodiversityR'' and "vegan" libraries in R Studio software.

Finally, to assess similarity in community structure across sampling stations, a hierarchical cluster analysis was performed. Microphytoplankton abundance data were square-root-transformed before analysis to mitigate the influence of dominant taxa and enhance the statistical contribution of rare species (Clarke & Warwick 2003). Similarity between stations was then determined using the Bray-Curtis coefficient; this metric is widely preferred in marine ecological studies because it effectively accounts for both community composition and relative abundance, while remaining insensitive to joint absences (Legendre & Legendre 2012).

The vertical hydrographic profiles recorded at each sampling station revealed distinct thermal and chemical stratification. Across all sites, surface temperatures

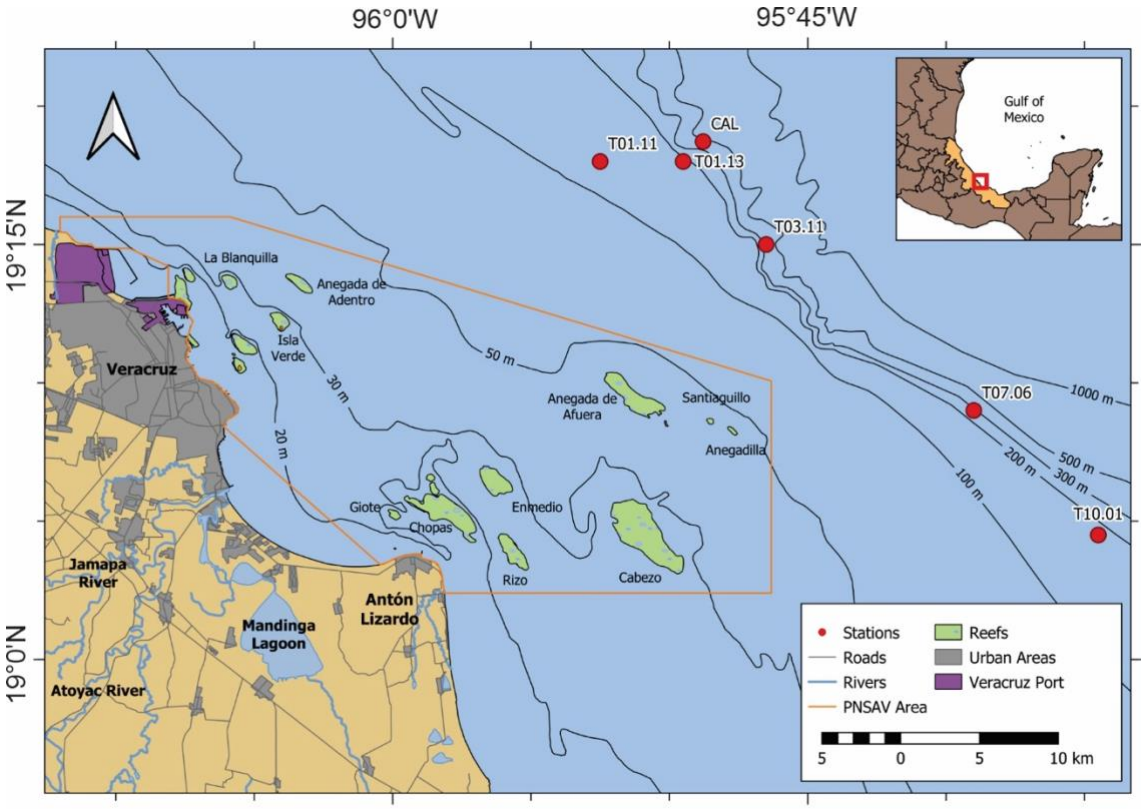

Figure 1. The study area is located off the coast of Veracruz in the southwestern Gulf of Mexico. Red points denote sampling stations where high-resolution hydrographic data and water samples for microphytoplankton analysis were collected. The stations are situated along the perimeter of the Veracruz Reef System, with the protected area boundaries delineated by the orange line.

remained relatively consistent, ranging from 24.1 to 24.9°C, then decreased steadily with depth. Dissolved oxygen (DO) concentrations were generally uniform at approximately 200 µmol kg^{-1} within the mixed layer, with only minor variations occurring beneath the thermocline and pycnocline boundaries.

The depths of the thermocline and pycnocline varied significantly between the northern and southern stations, ranging from 80 to 140 m, with an overall mean depth of 101.7 m. The standard deviation is 21.37 m, reflecting the significant spatial variability in the region.

At station CAL (Fig. 2a), the thermocline was established at 80 m, accompanied by a chlorophyll-*a* (Chl-*a*) distribution with two peaks reaching 0.48 mg m^{-3}. In contrast, station T10.01 (Fig. 2b) exhibited the deepest thermocline among all sites at 140 m; here, Chl-*a* was uniformly distributed throughout the water column at concentrations near 0.5 mg m^{-3}. At station T07.06 (Fig. 2c), the thermocline/pycnocline depth was recorded at 110 m, with a Chl-*a* maximum (0.31 mg m^{-3}) concentrated in a shallow layer between 15 and 25 m.

Stations T03.11, T01.13, and T01.11 showed intermediate stratification depths of 90-100 m. At T03.11 (Fig. 2d) and T01.13 (Fig. 2e), the thermocline was observed at 90 m, with distinct Chl-*a* peaks of 0.33 mg m^{-3} occurring in layers at 68 and 70 m, respectively. Finally, station T01.11 (Fig. 2f) showed the thermocline and pycnocline at 100 m, characterized by a Chl-*a* distribution with several crests, with a maximum concentration of 0.30 mg m^{-3} at a depth of 62 m.

Chl-*a* concentrations across the stations exhibit significant spatial variability in both magnitude and vertical structure. The maximum concentrations range from 0.30 mg m^{-3} at station T01.11 to 0.50 mg m^{-3} at station T10.01, with the latter notable for its uniform distribution across the water column. In contrast to this uniform profile, other stations display more structured layering; for instance, CAL shows two peaks reaching 0.48 mg m^{-3}, while stations T03.11 and T01.13 exhibit consistent, distinct peaks of 0.33 mg m^{-3} at depths near 70 m. Station T07.06 represents a unique case where the maximum concentration of 0.31 mg m^{-3} is confined

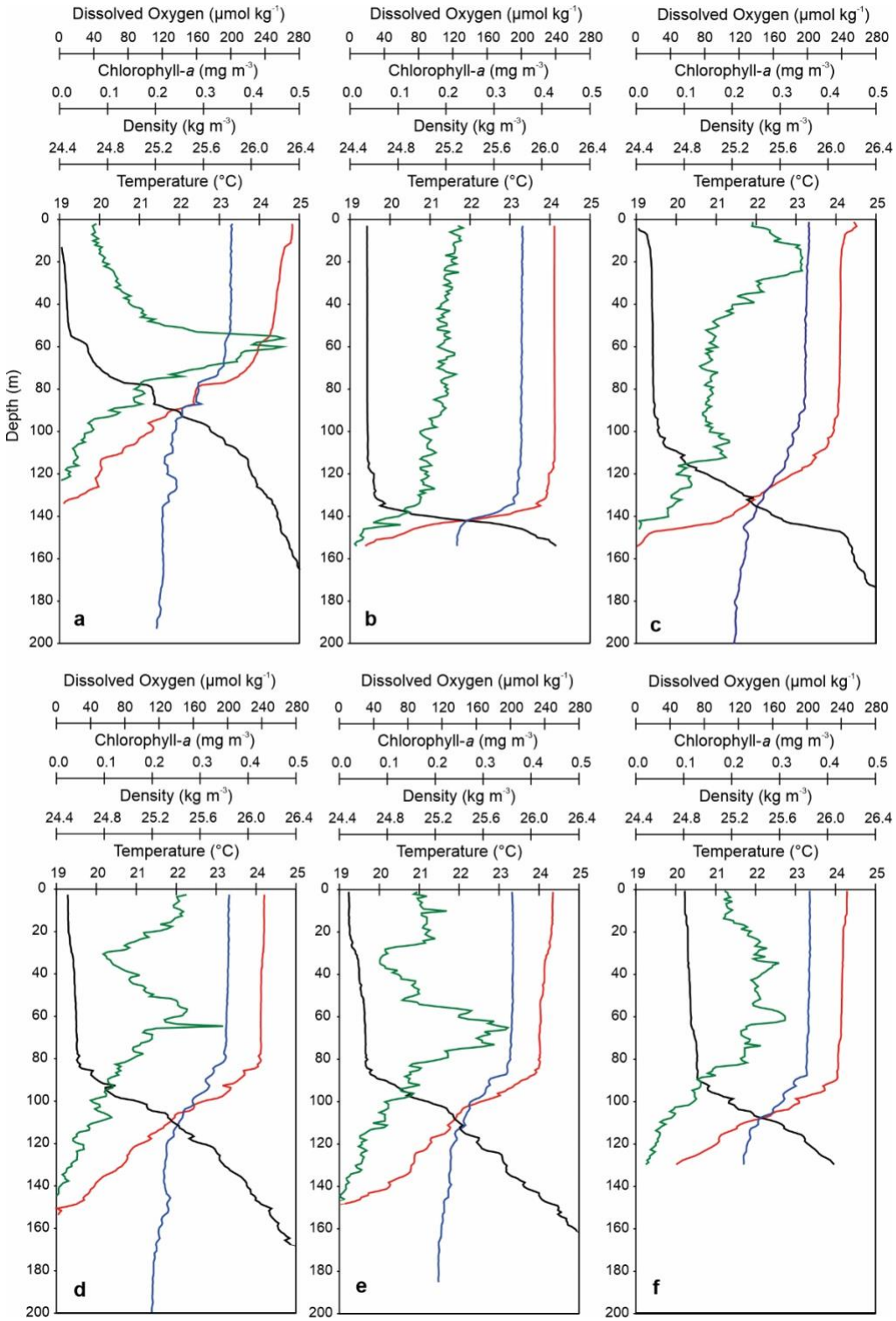

Figure 2. Vertical profiles of the hydrographic variables across all sampling points. The red line represents the vertical distribution of temperature (°C). The black line represents the vertical distribution of density (kg m^{-3}). The blue line represents the vertical distribution of dissolved oxygen (µmol kg^{-1}), and the green line represents the vertical distribution of chlorophyll-*a* (mg m^{-3}). Sampling stations: a) CAL, b) T10.01, c) T07.06, d) T03.11, e) T01.13 and f) T01.11.

to a shallow layer between 15 and 25 m, diverging from the intermediate stratification depths of 90-100 m observed at the other sampling stations.

A total of 110 microphytoplankton species were identified, which included 1 ciliate, 2 cyanobacteria, 57 diatoms, 48 dinoflagellates, and 2 silicoflagellates. Among these groups, diatoms were the most abundant, with 20,060 cells L^{-1}, followed by dinoflagellates at 17,720 cells L^{-1}. Silicoflagellates were the least abundant, totaling 760 cells L^{-1}. The most abundant species included the ciliate *Mesodinium rubrum* (3,460 cells L^{-1}), the cyanobacteria *Trichodesmium hildebrandtii* (2,160 cells L^{-1}), the diatom *Pseudo-nitzschia pseudodelicatissima* (3,600 cells L^{-1}), the dinoflagellate *Heterocapsa orientalis* (1,960 cells L^{-1}), and the silicoflagellate *Dictyocha fibula* (540 cells L^{-1}) (Table 1).

Regarding relative abundance, the community was dominated by diatoms (51.81%) and dinoflagellates (43.63%), while cyanobacteria and silicoflagellates each comprised 1.81%. Ciliates represented a minor portion of the total community, contributing only 0.94%.

The ecological indices calculated in this study indicate high biodiversity. The Margalef species richness index was 10.17, while the Shannon-Weaver index was 4.03. These values highlight the significant species richness and diversity within the thermocline, underscoring the ecological importance of this layer.

Hierarchical cluster analysis, performed using the Bray-Curtis similarity index on square-root transformed data, identified distinct spatial groupings among the sampling stations (Fig. 3). A primary cluster exhibiting the highest affinity was formed by stations T01.11 and T03.11 (~58% similarity). A secondary, well-defined group emerged between stations CAL and T10.01 (~52% similarity). In contrast, station T07.06 markedly diverged from the remaining sites, joining the dendrogram at a similarity level below 46%. This segregation reflects a heterogeneous biological community structure, likely driven by the specific hydrographic conditions or distinct water masses encountered during the cruise.

The thermocline is a dynamic temperature gradient that separates warm surface water from colder deep layers, shifting with seasonal heating and wind-driven mixing. This physical stratification serves as a critical ecological boundary that fundamentally shapes the structure and distribution of phytoplankton communities (Pedlosky 2006, Mena et al. 2019).

The vertical hydrographic profiles in our study revealed a deep thermocline and pycnocline, situated between 80 and 140 m. This depth range aligns with previous observations in the Gulf of Mexico during "Nortes" events (e.g. López-Cabello et al. 2025, Durán-Campos et al. 2025). This deepened state is a characteristic regional response driven by two primary mechanisms: surface cooling and mechanical wind stress. First, the reduction in sea surface temperatures induces vertical convective mixing, which effectively depresses the thermocline. Second, during these periods, the southwestern gulf experiences intense wind speeds, often exceeding 100 km h^{-1} (Salas-Monreal et al. 2022). These winds generate vertical mixing, further deepening both the thermocline and the pycnocline throughout the water column.

The deepening of the thermocline in response to wind-driven winter storms is a globally recognized phenomenon, documented in regions such as the Gulf of Tehuantepec (Trasviña et al. 1995), the southwestern Indian Ocean (Manola et al. 2015), and the South China Sea (Liu et al. 2023). These studies highlight how intense wind stress facilitates vertical mixing within the surface layer, physically forcing the thermocline to greater depths.

Such fluctuations in thermocline depth directly influence the structure of phytoplankton communities (Whang et al. 2024). In the present study, taxonomic analysis revealed high species richness (110 species), consistent with regional records (e.g. Okolodkov et al. 2011). Notably, our findings identify the thermocline as a critical stratum for microphytoplankton diversity in the coastal waters off Veracruz, an ecological feature of this region that has not been previously characterized. It is important to note that the ecological indices calculated in our study were consistently high. These values align with those documented in other highly diverse marine environments, such as the Red Sea ($D_{Mg} = 6.18$) (Al-Mur 2024) and Xiamen, China ($D_{Mg} = 9.2$) (Chen et al. 2010), reinforcing the status of the thermocline as a site of significant biological complexity.

In this study, *Pseudo-nitzschia pseudodelicatissima* was the most abundant diatom, with concentrations reaching 3,600 cells L^{-1} (Table 1). Similar values have been documented at thermocline depths in the Black Sea, where they were driven by increased nutrient availability (Lifanchuk et al. 2023). Although direct nutrient concentrations were not measured, we hypothesize that intense, wind-driven mixing events facilitated the vertical transport of nutrients from deeper layers into the surface and subsurface strata (including the thermocline), thereby sustaining the observed phytoplankton population peaks.

Table 1. Taxonomic composition of microphytoplankton communities and their total abundance (cells L^{-1}) associated with deep thermoclines off the coast of Veracruz, southwestern Gulf of Mexico, during a "Nortes" storm season.

Taxa	Sampling station						Total abundance (ind 100 m^{-3})
	T01.11	T01.13	CAL	T03.11	T07.06	T10.01	
Ciliates							
Mesodinium rubrum (Lohmann) Hamburger & Buddenbrock, 1911	500	620	1000	820	220	300	3460
Cyanobacteria							
Trichodesmium hildebrandtii Gomont, 1892	200	260	600	540	160	400	2160
Trichodesmium erythraeum Ehrenberg ex Gomont, 1892	0	200	300	200	0	200	900
Diatoms							
Actinoptychus adriaticus Grunow, 1863	0	200	0	0	0	0	200
Actinocyclus octonarius Ehrenberg, 1837	100	0	100	100	80	200	580
Actinoptychus senarius (Ehrenberg) Ehrenberg, 1843	200	100	0	40	40	100	480
Alveus marinus (Grunow) Kaczmarska & Fryxell, 1996	100	40	0	100	80	0	320
Asteromphalus arachne (Brébisson) Ralfs, 1861	100	0	200	0	0	200	500
Asteromphalus cleveanus Grunow, 1876	300	0	0	200	160	300	960
Asteromphalus roperianus (Greville) Ralfs, 1861	0	0	0	0	20	0	20
Azpeitia nodulifera (A.W.F. Schmidt) G.A. Fryxell & P.A. Sims, 1986	300	100	100	100	0	0	600
Bacteriastrum hyalinum Lauder, 1864	0	0	0	100	0	0	100
Chaetoceros affinis Lauder, 1864	0	0	0	0	40	0	40
Chaetoceros aequatorialis Cleve, 1901	0	0	100	0	0	100	200
Chaetoceros decipiens Cleve, 1873	100	0	0	40	40	0	180
Chaetoceros mannaii Y. Li, Boonprakob, Moestrup & Lundholm, 2018	0	100	0	0	0	0	100
Chaetoceros peruvianus Brightwell, 1856	100	0	200	0	0	0	300
Chaetoceros socialis H.S. Lauder, 1864	0	40	0	40	40	0	120
Chaetoceros willei Gran, 1897	100	0	0	40	0	0	140
Coscinodiscus asteromphalus Ehrenberg, 1844	100	200	100	200	120	100	820
Coscinodiscus wailesii Gran & Angst, 1931	100	200	100	100	80	0	580
Corethron pennatum (Grunow) Ostenfeld, 1902	40	0	0	0	0	0	40
Cyclotella litoralis Lange & Syvertsen, 1989	200	0	100	100	40	200	640
Cyclotella stylorum Brightwell, 1860	0	0	100	0	0	0	100
Cylindrotheca closterium (Ehrenberg) Reimann & J.C. Lewin, 1964	100	0	0	200	100	0	400
Dactyliosolen fragilissimus (Bergon) Hasle, 1996	0	0	0	0	0	100	100
Detonula moseleyana (Castracane) H.H. Gran, 1900	0	0	0	0	100	100	200
Detonula pumila (Castracane) Gran, 1900	0	0	0	0	40	0	40
Entomoneis alata (Ehrenberg) Ehrenberg, 1845	0	0	0	0	40	0	40
Fragilariopsis doliolus (Wallich) Medlin & P.A. Sims, 1993	0	40	0	40	0	0	80
Grammatophora marina (Lyngbye) Kützing, 1844	0	0	0	0	0	100	100
Guinardia striata (Stolterfoth) Hasle, 1996	200	100	0	200	0	0	500
Haslea trompii (Cleve) Simonsen, 1974	200	100	300	200	260	0	1060
Haslea wawrikae (Hustedt) Simonsen, 1974	0	0	0	40	0	0	40
Hemiaulus membranaceus Cleve, 1873	100	0	0	0	0	0	100
Hemidiscus cuneiformis Wallich, 1860	100	100	0	0	0	0	200
Leptocylindrus danicus Cleve, 1889	100	40	0	0	0	0	140
Mastogloia minuta Greville, 1857	0	0	0	0	0	40	40
Navicula distans (W. Smith) Brébisson, 1854	0	0	0	0	100	0	100
Neodelphineis indica (F.J.R. Taylor) Y. Tanimura, 1992	200	0	0	0	0	0	200
Nitzschia bicapitata Cleve, 1901	100	100	200	200	80	200	880
Nitzschia longissima (Brébisson ex Kützing) Grunow, 1862	0	100	0	0	0	0	100
Planktoniella muriformis (Loeblich III, W.W. Wight & W.M. Darley) Round, 1972	420	0	0	100	0	0	520
Planktoniella sol (G.C. Wallich) Schütt, 1892	0	0	200	100	40	100	440
Pleurosigma fasciola (Ehrenberg) W. Smith, 1852	0	0	0	0	40	0	40
Pleurosigma nicobaricum Grunow, 1880	0	400	0	0	0	0	400
Pleurosigma normanii Ralfs, 1861	100	0	0	100	0	0	200

Continuation

Taxa	Sampling station						Total abundance (ind 100 m^{-3})
	T01.11	T01.13	CAL	T03.11	T07.06	T10.01	
Pleurosigma salinarum (Grunow) Grunow, 1880	100	80	100	0	0	200	480
Pseudo-nitzschia pseudodelicatissima (Hasle) Hasle, 1993	1100	700	1000	100	500	200	3600
Pseudo-nitzschia pungens (Grunow ex Cleve) Hasle, 1993	100	500	100	0	0	200	900
Pseudo-nitzschia roundii D.U. Hernández-Becerril, l 2006	200	0	100	0	0	0	300
Pseudo-nitzschia subfraudulenta (Hasle) Hasle, 1993	0	0	100	0	0	0	100
Pseudo-nitzschia subpacifica (Hasle) Hasle, 1993	0	0	100	0	0	0	100
Rhizosolenia hyalina Ostenfeld, 1901	0	0	100	0	0	0	100
Stigmaphora rostrata Wallich, 1860	0	0	0	40	0	0	40
Thalassionema nitzschioides (Grunow) Mereschkowsky, 1902	0	20	200	40	0	0	260
Thalassionema frauenfeldii (Grunow) Tempère & Peragallo, 1910	100	0	100	0	0	0	200
Thalassiosira leptopus (Grunow) Hasle & G. Fryxell, 1977	100	0	0	0	40	0	140
Thalassiosira tenera Proshkina-Lavrenko, 1961	100	40	400	100	20	200	860
Thalassiosira punctifera (Grunow) Fryxell, Simonsen & Hasle, 1974	0	0	0	0	40	0	40
Dinoflagellates							
Achradina pulchra Lohmann, 1903	0	0	100	800	140	200	1240
Akashiwo sanguinea (K. Hirasaka) Gert Hansen & Moestrup, 2000	0	40	0	0	0	0	40
Azadinium poporum Tillmann & Elbrächter, 2011	100	0	0	200	0	0	300
Blepharocysta denticulata D.-S. Nie, 1939	420	120	0	220	60	200	1020
Corythodinium biconicum (Kofoid) F.J.R. Taylor, 1976	0	0	200	0	200	0	400
Corythodinium mucronatum (B. Hope) F. Gómez, 2017	400	0	0	0	0	0	400
Corythodinium reticulatum (Stein) F.J.R. Taylor, 1976	0	0	0	0	40	0	40
Cucumeridinium lira (Kofoid & Swezy) F. Gómez, P. López-García, H. Takayama & D. Moreira, 2015	0	100	0	0	0	0	100
Diplopelta globula (T.H. Abé) Balech, 1979	0	0	100	0	0	0	100
Gonyaulax areolata Kofoid & J.R. Michener, 1911	0	0	140	0	0	0	140
Gymnodinium catenatum H.W. Graham, 1943	200	100	0	100	0	0	400
Gyrodinium fusiforme Kofoid & Swezy, 1921	0	200	200	400	0	200	1000
Gyrodinium pepo (F. Schütt) Kofoid & Swezy, 1921	0	40	0	0	0	0	40
Gyrodinium spirale (Bergh) Kofoid & Swezy, 1921	0	100	0	0	0	0	100
Heterocapsa niei (A.R. Loeblich) L.C. Morrill & A.R. Loeblich 1981	100	0	100	200	0	0	400
Heterocapsa orientalis Iwataki, Botes & Fukuyo, 2003	400	500	400	240	120	300	1960
Kapelodinium vestifici (Schütt) Boutrup, Moestrup & Daugbjerg, 2016	0	400	100	40	0	0	540
Karenia brevisulcata (F.H. Chang) Gert Hansen & Moestrup, 2000	100	0	0	0	40	100	240
Lingulaulax polyedra (F. Stein) M.J. Head, K.N. Mertens & R.A. Fensome, 2024	0	0	0	0	0	200	200
Oxyphysis oxytoxoides Kofoid, 1926	0	100	0	0	0	0	100
Oxytoxum mediterraneum Schiller, 1937	0	0	100	100	0	0	200
Oxytoxum scolopax F. Stein, 1883	200	0	0	200	0	0	400
Oxytoxum variabile J. Schiller, 1937	0	0	0	200	0	0	200
Podolampas palmipes F. Stein 1883	0	0	0	0	0	100	100
Polykrikos hartmannii W.M. Zimmermann, 1930	0	100	0	0	0	0	100
Pronoctiluca spinifera (Lohmann) Schiller, 1932	0	0	100	0	0	0	100
Prorocentrum compressum (Bailey) T.H. Abé ex J.D. Dodge, 1975	0	0	0	0	40	0	40
Prorocentrum gracile F. Schütt, 1895	0	0	100	20	0	0	120
Prorocentrum koreanum M.-S. Han, S.Y. Cho & P. Wang, 2016	200	0	0	0	0	300	500

Continuation

Taxa	Sampling station						Total abundance (ind 100 m^{-3})
	T01.11	T01.13	CAL	T03.11	T07.06	T10.01	
Prorocentrum lenticulatum (Matzenauer) F.J.R. Taylor, 1976	0	100	0	0	40	0	140
Prorocentrum obtusidens J. Schiller, 1928	200	100	100	100	200	400	1100
Prorocentrum robustum B.F. Osorio, 1942	0	0	0	100	0	0	100
Prorocentrum sigmoides Böhm, 1933	0	0	0	100	40	0	140
Protoperidinium corniculum (Kofoid & J.R. Michener) F.J.R. Taylor & Balech, 1988	0	0	100	0	0	0	100
Protoperidinium pentagonum (Gran) Balech, 1974	0	0	0	0	60	0	60
Protoperidinium punctulatum (Paulsen) Balech, 1974	200	100	400	200	300	200	1400
Protoperidinium robustum (Meunier) Hernández-Becerril, 1991	500	100	300	200	360	100	1560
Protoperidinium saltans (Meunier) Balech, 1973	0	0	0	0	60	0	60
Protoperidinium spirale (Gaarder, 1954) Balech, 1974	0	0	0	0	40	0	40
Protoperidinium tuba (J. Schiller) Balech, 1974	0	0	200	0	0	0	200
Pyrocystis lunula (F. Schütt) F. Schütt, 1896	0	40	0	0	0	0	40
Pyrophacus steinii (Schiller) Wall & Dale, 1971	0	0	0	0	100	0	100
Scrippsiella acuminata (Ehrenberg) Kretschmann, Elbrächter, Zinssmeister, S. Soehner, Kirsch, Kusber & Gottschling, 2015	0	100	0	0	0	0	100
Triadinium polyedricum (Pouchet) Dodge, 1981	600	100	100	500	80	100	1480
Tripos carriensis (Gourret) Hallegraeff & Huisman, 2013	0	0	0	0	40	0	40
Tripos furca (Ehrenberg) F. Gómez, 2013	200	100	100	0	0	0	400
Tripos longirostrum (Gourret) Hallegraeff & Huisman, 2020	0	0	0	0	0	100	100
Tripos teres (Kofoid) F. Gómez, 2013	0	0	40	0	0	0	40
Silicoflagellates							
Dictyocha fibula Ehrenberg, 1839	200	100	0	40	100	100	540
Octactis octonaria (Ehrenberg) Hovasse, 1946	200	0	0	0	20	0	220
Total abundance (ind 100 m^{-3})	**10180**	**7020**	**8980**	**8140**	**4600**	**6140**	**45060**

Regarding dinoflagellates, *Heterocapsa orientalis* was the most abundant species recorded in our study. Recent research in the Campeche Canyon, southern Gulf of Mexico, has also associated this species with deep Chl-*a* maxima occurring alongside deep thermoclines (e.g. Durán-Campos et al. 2025). However, *H. orientalis* was not the primary dominant species in their study; its prevalence here reinforces the observation that this taxon is typically distributed at significant depths within the water column.

Consistent with our results, high abundances of *Mesodinium rubrum* have been frequently associated with thermocline and pycnocline oscillations. In the Gulf of Finland, for instance, blooms of this species are linked to thermocline fluctuations that modulate nutrient availability (Lips & Lips 2017), a pattern also observed along the northern coast of Brazil (Owen et al. 1992). Winter conditions in the Gulf of Mexico typically enhance nutrient availability, a known driver of this species' proliferation (Durán-Campos et al. 2025). This nutrient enrichment could contribute to the abundance values observed in our study; however, the unique trophic role of *M. rubrum* warrants consideration. As a mixotrophic ciliate that actively preys on phytoplankton, its high abundance may reflect a synergistic response to both increased nutrient-driven primary productivity and the resulting rise in available prey (Labucis et al. 2023).

The results presented here provide a novel characterization of microphytoplankton taxonomic composition associated with deep thermoclines, a relationship previously unaddressed off the coast of Veracruz in the southwestern Gulf of Mexico. These findings are significant as regional shifts in thermal stratification fundamentally alter the physical structure of the water column. Understanding the vertical distribution of microphytoplankton is critical because the thermocline acts as a physical barrier that aggregates organisms, creating localized hotspots for primary production and nutrient cycling. Consequently, these deep-seated communities play a vital role in local carbon fixation and the overall energy flux within the

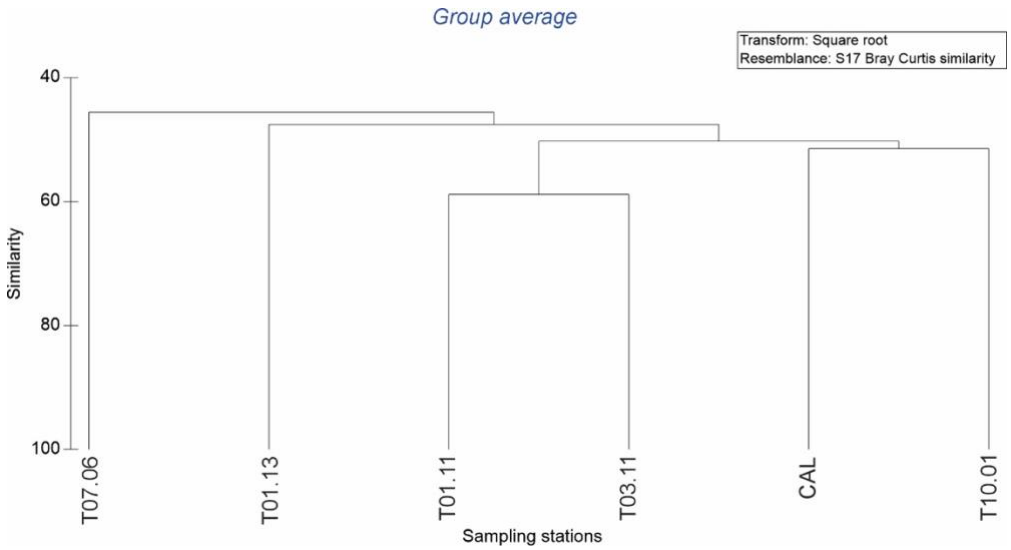

Figure 3. Hierarchical cluster analysis performed using the Bray-Curtis similarity index on square-root transformed data.

pelagic ecosystem. These results provide essential baseline data for assessing how regional environmental variability influences community structure and biological productivity in this specific marine area.

Credit author contribution

All authors contributed equally to this study. All authors have read and accepted the published version of the manuscript.

Conflict of interest

The authors declare no conflict of interest.

ACKNOWLEDGMENTS

The authors deeply appreciate the assistance of the captain and crew of the R/V Justo Sierra, as well as many students who participated in the research cruise ACGOM-1. Francisco Ponce Núñez and Sergio Castillo Sandoval provided technical support during analyses. The Instituto de Ciencias del Mar y Limnología, UNAM, funded this study. UNAM funded the ship time for the research cruise aboard the R/V Justo Sierra. We thank the three anonymous reviewers for their insightful comments, which significantly improved this manuscript.

REFERENCES

Al-Mur, B.A. 2024. Environmental assessment using phytoplankton diversity, nutrients, chlorophyll-*a*, and trophic status along southern coast of Jeddah, Red Sea. Journal of Marine Science and Engineering, 13: 29. doi: 10.3390/jmse13010029

Alvarez, I., Rasmuson, L.K., Gerard, T., et al. 2021. Influence of the seasonal thermocline on the vertical distribution of larval fish assemblages associated with Atlantic bluefin tuna spawning grounds. Oceans, 2: 64-83. doi: 10.3390/oceans2010004

Carter, R.A., McMurray, H.F. & Largier, J.L. 2010. Thermocline characteristics and phytoplankton dynamics in Agulhas Bank waters. South Africa Journal of Marine Science, 5: 327-336. doi: 10.2989/02577618 7784522306

Clarke, K.R. & Warwick, R.M. 2003. A taxonomic distinctness index and its statistical properties. Journal of Applied Ecology, 35: 523-531. doi: 10.1046/j.1365-2664.1998.3540523.x

Chen, B., Xu, Z., Zhou, Q., et al. 2010. Long-term changes of phytoplankton community in Xiagu waters of Xiamen, China. Acta Oceanologica Sinica, 2: 104-114. doi: 10.1007/s13131-010-0081-4

Cupp, E.E. 1943. Marine plankton diatoms of the west coast of North America. University of California Press, Berkeley.

Durán-Campos, E., Salas de León, D.A., Monreal-Gómez, M.A., et al. 2017. Patterns of chlorophyll-a distribution linked to mesoscale structures in two contrasting areas, Campeche Canyon and Bank, southern Gulf of Mexico. Journal of Sea Research, 123: 30-38. doi: 10.1016/j.seares.2017.03.013

Durán-Campos, E., Salas-de-León, D.A., Monreal-Gómez, M.A., et al. 2025. Phytoplankton assemblage in the Campeche Canyon (southern Gulf of Mexico) and its relationship with hydrography during a "Nortes" storm season. Phycology, 5: 86. doi: 10.3390/phycology 5040086

Edler, L. & Elbrachter, M. 2010. The Utermöhl method for quantitative phytoplankton analysis. In: Karlson, B., Cusack, C. & Bresnan, E. (Eds.). Microscopic and molecular methods for quantitative phytoplankton analysis. Intergovernmental Oceanographic Commission of UNESCO, Potsdam, pp. 13-20.

González-Fernández, J.M., Luna-Soria, R., Alexander-Valdés, H., et al. 2025. Influence of mesoscale eddies on the spring phytoplankton groups in the southern Gulf of Mexico. Botanica Marina, 68: 85-99. doi: 10.1515/bot-2024-0042

Grigoratou, M., Menden-Deuer, S., McQuatters-Gollop, A., et al. 2025. The immeasurable value of plankton to humanity. BioScience, 75: 706-721. doi: 10.1093/biosci/biaf049

Hickman, A.E., Hooligan, P.M., Moore, C.M., et al. 2009. Distribution and chromatic adaptation of phytoplankton within a shelf sea thermocline. Limnology and Oceanography, 54: 525-536. doi: 10.4319/lo.2009.54.2.0525

Komárek, J. & Anagnostidis, K. 1986. Modern approach to the classification system of cyanophytes (Croococcales). Archiv für Hydrobiologie Supplement, 43: 157-226.

Labucis, A., Labuce, A., Jurgensone, I., et al. 2023. A. Seasonal variation in size structure and production of autotrophic plankton community in eutrophied, low-light environment: A focus on *Mesodinium rubrum*. Oceanologia, 65: 398-409. doi: 10.1016/j.oceano.2022.11.003

Legendre, P. & Legendre, L. 2012. Numerical ecology. Elsevier, Amsterdam.

Licea, S., Luna, R., Okolodkov, Y.B., et al. 2017. Phytoplankton abundance and distribution on the Yucatan shelf (June 1979 and April 1983). Novosti Sistematiki Nizaikh Rastenii, 51: 121-144.

Licea, S., Zamudio, M.E., Luna, R., et al. 2004. Free-living dinoflagellates in the southern Gulf of Mexico: Report of data (1979-2002). Phycological Research, 52: 419-428.

Licea, S., Zamudio, M.E., Moreno-Ruiz, J.L., et al. 2011. A suggested local region in the Southern Gulf of Mexico using a diatom database (1979-2002) and oceanic hydrographic features. Journal of Environmental Biology, 32: 443-453.

Lifanchuk, A.V., Mikaelyan, A.S., Sergeeva, A.V., et al. 2023. Seasonal dynamics and ecology of the *Pseudo-nitzschia delicatissima* group in the Black Sea. Regional Studies in Marine Science, 68: 103249. doi: 10.1016/j.rsma.2023.103249

Lips, I. & Lips, U. 2017. The importance of *Mesodinium rubrum* at post-spring bloom nutrient and phytoplankton dynamics in the vertically stratified Baltic Sea. Frontiers in Marine Science, 4: 407. doi: 10.3389/fmars.2017.00407

Liu, Q., Chen, J., Jin, H., et al. 2023. Deepening of the thermocline increases primary production in winter vs summer in the northern South China Sea. Deep Sea Research I, 201: 104163. doi: 10.1016/j.dsr.2023.104163

López-Cabello, Z., Coria-Monter, E., Monreal-Gómez, M.A., et al. 2025. Vertical assemblage of the holoplanktonic mollusks (Pteropoda and Pterotracheoidea: Carinaiidae, Pterotracheidae) in the Campeche Canyon, southern Gulf of Mexico, during a "Nortes" season. PeerJ, 13: e19118. doi: 10.7717/peerj.19118

Magurran, A. 2004. Measuring biological diversity. Blackwell, Oxford.

Manola, I., Selten, F.M., de Ruijter, W.P.M., et al. 2015. The ocean-atmosphere response to wind-induced thermocline changes in the tropical south western Indian Ocean. Climate Dynamics, 45: 989-1007. doi: 10.1007/s00382-014-2338-7

Margalef, R. 1969. Diversity and stability: A practical proposal and a model of interdependence. Brookhaven Symposia in Biology, 22: 25-37.

Mena, C., Reglero, P., Hidalgo, M., et al. 2019. Phytoplankton community structure is driven by stratification in the oligotrophic Mediterranean Sea. Frontiers in Microbiology, 10: 1698. doi: 10.3389/fmicb.2019.01698

Okolodkov, Y.B. 2008. *Protoperidinium* Bergh (Dinophyceae) of the National Park Sistema Arrecifal Veracruzano, Gulf of Mexico, with a key for identification. Acta Botanica Mexicana, 84: 93-149.

Okolodkov, Y.B. 2010. *Ceratium* Schrank (Dinophyceae) of the National Park Sistema Arrecifal Veracruzano, Gulf of Mexico, with a key for identification. Acta Botanica Mexicana, 93: 41-101.

Okolodkov, Y.B. 2014. Dinophysiales (Dinophyceae) of the National Park Sistema Arrecifal Veracruzano, Gulf of Mexico, with an identification key. Acta Botanica Mexicana, 106: 9-71.

Okolodkov, Y.B., Aké-Castillo, J.A., Gutiérrez-Quevedo, M.G., et al. 2011. Annual cycle of the plankton

biomass in the National Park Sistema Arrecifal Veracruzano, southwestern Gulf of Mexico. In: Kattel, G. (Ed.). Zooplankton and phytoplankton: Types, characteristics, and ecology. Nova Science Publishers, New York, pp. 63-88.

Ortiz-Burgos, S. 2016. Shannon-Weaver diversity index. In: Kennish, M.J. (Ed.). Encyclopedia of estuaries. Encyclopedia of Earth Sciences Series. Springer, Dordrecht.

Owen, R.W., Gianesella-Galvao, S.F. & Kutner, M.B.B. 1992. Discrete, subsurface layers of the autotrophic ciliate *Mesodinium rubrum* off Brazil. Journal of Plankton Research, 14: 97-105.

Pedlosky, J. 2006. A history of thermocline theory. In: Jochum, M. & Murtugudde, R. (Eds.). Physical oceanography: Developments since 1950. Springer Science, New York, pp. 139-152.

Reynolds, C.S. 2006. The ecology of phytoplankton. Cambridge University Press, Cambridge.

Salas-Monreal, D., Monreal-Jiménez, R., Contreras-Tereza, K., et al. 2022. Hydrographic variation in a tropical coral reef system: The Veracruz Reef System, Gulf of Mexico. Oceanologia, 64: 473-488. doi: 10.1016/j.oceano.2022.03.002

Salas-Monreal, D., Valle-Levinson, A. & Athie, G. 2019. Flow modifications over a tropical coral reef system. Estuarine, Coastal and Shelf Science, 217: 271-280. doi: 10.1016/j.ecss.2018.11.029

Salas-Perez, J.J. & Granados-Barba, A. 2008. Oceanographic characterization of the Veracruz reef system. Atmósfera, 21: 281-301.

Sharples J., Moore, M., Rippeth, T.P., et al. 2001. Phytoplankton distribution and survival in the thermocline. Limnology and Oceanography, 46: 486-496. doi: 10.4319/lo.2001.46.3.0486

Received: January 19, 2026; Accepted: March 5, 2026

Siegel, D.A., DeVries, T., Cetinic, I., et al. 2023. Quantifying the ocean's biological pump and its carbon cycle impacts on global scales. Annual Review of Marine Science, 15: 329-356. doi: 10.1146/annurev-marine-040722-115226

Throndsen, J. 1997. The planktonic marine flagellates. In: Tomas, C.R. (Ed.). Identifying marine phytoplankton. Academic Press, San Diego, pp. 591-729.

Throndsen, J., Hasle, G.R. & Tangen, K. 2003. Norsk kystplankton flora. Almater Forlag As, Oslo.

Tomas, C.R. 1997. Identifying marine phytoplankton. Academic Press, San Diego.

Trasviña, A., Barton, E.D., Brown, J., et al. 1995. Offshore wind forcing in the Gulf of Tehuantepec, Mexico: The asymmetric circulation. Journal of Geophysical Research Oceans, 100: 20649-20663. doi: 10.1029/95JC01283

Vajravelu, M., Martin, Y., Ayyappan, S., et al. 2017. Seasonal influence of physicochemical parameters on phytoplankton diversity, community structure, and abundance at Parangipettai coastal waters, Bay of Bengal, south east coast of India. Oceanologia, 60: 114-127. doi: 10.1016/j.oceano.2017.08.003

Vidussi, F., Claustre, H., Manca, B.B., et al. 2001. Phytoplankton pigment distribution in relation to upper thermocline circulation in the eastern Mediterranean Sea during winter. Journal of Geophysical Research, 106: 19939-19956. doi: 10.1029/1999JC000308

Wang, L., Liu, J., Bao, Z., et al. 2024. Predictable shifts in diversity and ecosystem function in phytoplankton and zooplankton communities along thermocline stratification intensity continua. Science of the Total Environment, 912: 16898. doi: 10.1016/j.scitotenv.2023.168981

Xu, K., Huang, R.X., Wang, W., et al. 2017. Thermocline Fluctuations in the Equatorial Pacific related to the two types of El Niño events. Journal of Climate, 30: 6611-6627. doi: 10.1175/JCLI-D-16-0291.1